

A FLAME MODEL FOR MELTING AND DRIPPING OF POLYMERS

S. R. Idelsohn^{1*}, J. Marti¹, E. Oñate¹, R. Rossi¹ and K.M. Butler²

¹International Center for Numerical Methods in Engineering (CIMNE)

Universidad Politécnic de Cataluña

Campus Norte UPC, 08034 Barcelona, Spain

e-mail: julio.marti@cimne.upc.edu, web page: <http://www.cimne.com/>

*ICREA Research Professor at CIMNE.

²National Institute of Standards and Technology (NIST),

Building and Fire Research Laboratory (BFRL),

100 Bureau Drive, Gaithersburg, MD 20899, U.S.A.

1 INTRODUCTION

The versatility of polymeric materials, as demonstrated in such features as high strength, low weight, ease of processing, and capability to form into complex shapes, have led to their widespread industrial application in aircraft structures, transportation vehicles, building construction, maintenance and finishing products, electronic boards, bioengineering, structural materials, and many other different applications. Their behavior in a fire is of considerable interest because they play an important role in the ignition and growth stages of fire. In this paper, a new computational procedure for analysis of the combustion, melting and flame spread of polymers under fire conditions is presented. The method places the fluid as well as the solid problem into a Lagrangian framework [1]. This approach allows treatment of the whole domain, containing both fluid and solid subdomains which interact with each other, as a single entity and describes its behaviour by a single set of momentum, continuity and energy equations. The equations are discretized with the Particle Finite Element Method (PFEM) [2]. The paper is structured as follows. In the next section the basis of the PFEM is summarized. The essential governing equations and an overview of the discretization procedure and the general solution scheme are given. The potential of the PFEM to represent flaming combustion of polymers is shown in examples.

2 ABOUT THE PARTICLE FINITE ELEMENT METHOD

2.1 Basic concepts

In the PFEM the analysis domain is modeled with an updated Lagrangian formulation[2]. The analysis domain can include solid and fluid subdomains. As an example, we can model one or several thermoplastic objects and the surrounding air as comprising the analysis domain. All variables in the fluid and solid domains are assumed to be known in the current configuration at time t . The new set of variables in both domains is sought in the next configuration at time $t + \Delta t$. The FEM is used to solve the continuum equations in both domains. This requires a mesh discretizing these domains to be generated in order to solve the governing equations for both the fluid and solid problems in the standard FEM fashion. To do this, the nodes discretizing the analysis domain are treated as material particles whose motion is tracked during the transient solution. This is useful to model the separation of particles from a solid domain, such as in the dripping of melt particles from a thermoplastic object, and to follow their subsequent motion as individual

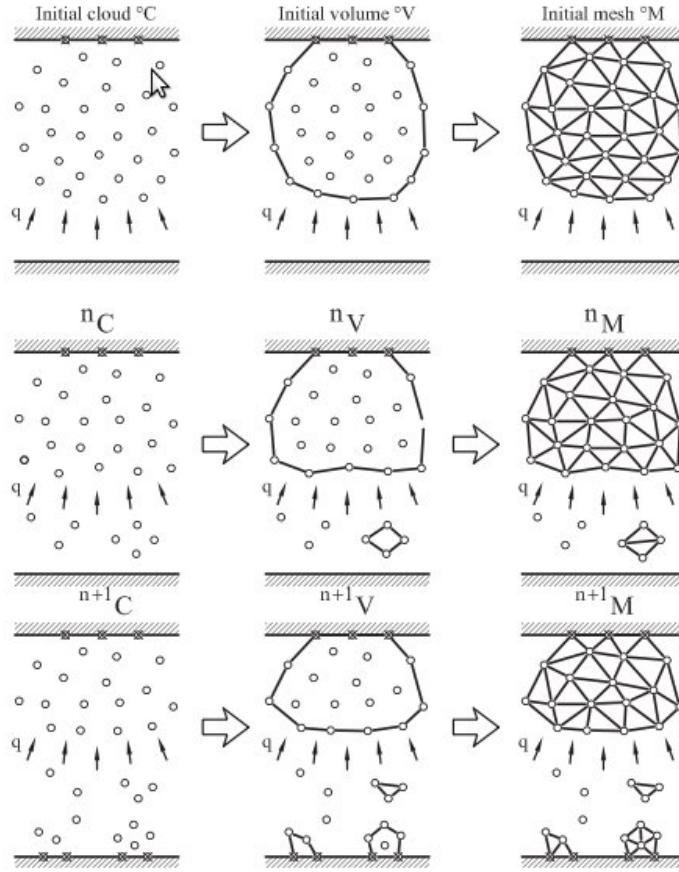


Figure 1: Polymer object subjected to a heat flux q applied to its lower boundary (arrows indicate incoming heat flux). Sequence of steps to update the cloud of nodes representing the object in time using the PFEM.

particles with a known density, an initial acceleration and velocity, and subject to gravity forces. Every node is a material point and hence is characterized by the density of the polymer material. The mass of a given domain is obtained by integrating the density at the different material points over the domain.

The way the PFEM solution process operates, for the problems we are solving in this paper, is schematically shown in Figure 1. The figure represents a polymer object hanging from a wall subjected to an incoming heat flux q acting at the lower part of the object. The collection or cloud of nodes pertaining to the polymer and the air analysis domain will be defined as (C), the volume defining the analysis domain as (V), and the mesh discretizing this domain as (M).

A typical solution with the PFEM involves the following steps:

1. The starting point at each time step is the cloud of points in the polymer and the air domain. For instance, 0C and nC are the clouds at the initial time and at time $t = t^n$, respectively (Figure 1).
2. Identify the boundaries defining the analysis domain, nV [3].
3. Discretize the analysis domain with a finite element mesh, nM .
4. Solve the coupled Lagrangian equations of motion for the domains. Compute the relevant state variables at the next (updated) configuration for $t + \Delta t$: velocities, strain rates, strains, pressure, viscous stresses, and temperature in the polymer.
5. Move the mesh nodes to a new position ${}^{n+1}C$, where $n + 1$ denotes the time $t^n + \Delta t$,

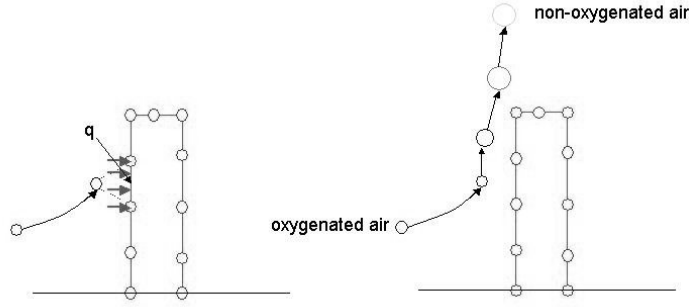


Figure 2: Illustration of flame algorithm.

in terms of the time increment size.

6. Go back to step 1 and repeat the solution process for the next time step. More details of the PFEM can be found in Refs. [4, 5].

2.2 Modeling of combustion with the PFEM

The gas phase particles originate as fully oxygenated air (100 % O_2). Figure 2 shows the approach of a gas phase particle to the thermoplastic object. When the air particle is close enough to contact a thermoplastic particle and the temperature of the thermoplastic particles exceeds a specified ignition temperature, several things happen. First, the high temperature causes gasification of the thermoplastic material, described by an Arrhenius expression. Mass lost from the condensed phase object becomes mass gained by the gas phase. Latent heat is absorbed during the phase change of material from liquid to gas, cooling the thermoplastic material. This is taken into account by the heat flux to the surface from the flame, which is fed by the fuel gases and is therefore proportional to the change in volume. During this encounter, the air particle loses some oxygen at a rate proportional to the stoichiometric ratio and the reaction rate, until after several contacts with the thermoplastic surface the oxygen is fully depleted. In an open space, the particle of non-oxygenated air rises away from the burning object. However, in an enclosed space, it will recirculate. The next time the particle encounters the fuel, no reaction will take place, and the flame may be extinguished.

3 GOVERNING EQUATIONS

Let $\Omega \subset \mathcal{R}^d$, $d \in \{2, 3\}$, be a bounded domain containing two subdomains with different materials (Figure 3). In our case, the subdomains are assumed to behave as viscous fluids. We denote time by t , the Cartesian spatial coordinates by $x = x_i|_{i=1}^d$, and the vectorial operator of spatial derivatives by $\nabla = \{\partial_{x_i}\}_{i=1}^d$. The evolution of the velocity $\mathbf{u} = \mathbf{u}(x, t)$, the pressure $p = p(x, t)$, the temperature $T = T(x, t)$ and the species $Y_k = Y_k(x, t)$ is governed by equations:

$$\frac{d\rho}{dt} + \rho \nabla \cdot \mathbf{u} = 0 \quad \text{in } \Omega \times (0, T) \quad (1)$$

$$\rho \frac{d\mathbf{u}}{dt} = \nabla \cdot \boldsymbol{\sigma} + \rho \mathbf{f} \quad \text{in } \Omega \times (0, T) \quad (2)$$

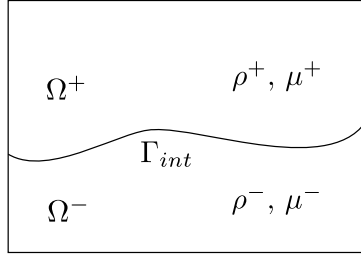


Figure 3: Two-fluid flow configuration.

$$\rho C \frac{dT}{dt} = \nabla \cdot (\kappa \nabla T) + Q \quad \text{in } \Omega \times (0, T) \quad (3)$$

$$\rho \frac{dY_k}{dt} = w_k + \nabla \cdot (\mathcal{D} \rho \nabla Y_k) \quad \text{in } \Omega^+ \times (0, T) \quad (4)$$

where ρ is the density, σ the Cauchy stress tensor, f the vector of gravity acceleration, C the heat capacity, κ the thermal conductivity, T the temperature, Q the heat source per unit volume, Y_k the mass fraction of species k , w_k the source term of species k , \mathcal{D} the diffusion coefficient and $d\phi/dt$ represents the total or material derivative of a function ϕ .

The constitutive equation for a Newtonian fluid is

$$\sigma = -p\mathbf{I} + 2\mu_f \mathbf{D} \quad (5)$$

where μ_f is the fluid viscosity, p is the thermodynamic (or hydrostatic) pressure of the fluid and \mathbf{D} is the deviatoric component of the symmetric part of the velocity gradient tensor \mathbf{L} . In our work the viscosity can be a function of temperature.

Let $\Gamma_{int}(t)$ be the interface that splits the domain Ω into two open subdomains, $\Omega^+(t)$ and $\Omega^-(t)$, which satisfy: $\Omega^+ \cap \Omega^- = \emptyset$, $\Omega = \bar{\Omega}^+ \cup \bar{\Omega}^-$, and $\Gamma_{int} = \bar{\Omega}^+ \cap \bar{\Omega}^- = \partial\Omega^+ \cap \partial\Omega^-$. In each subdomain, the physical properties are defined as:

$$\rho = \rho(\mathbf{x}, t) = \begin{cases} \rho^+ & \text{if } \mathbf{x} \in \Omega^+(t) \\ \rho^- & \text{if } \mathbf{x} \in \Omega^-(t) \end{cases}, \quad C = C(\mathbf{x}, t) = \begin{cases} C^+ & \text{if } \mathbf{x} \in \Omega^+(t) \\ C^- & \text{if } \mathbf{x} \in \Omega^-(t) \end{cases}, \quad (6)$$

$$\kappa = \kappa(\mathbf{x}, t) = \begin{cases} \kappa^+ & \text{if } \mathbf{x} \in \Omega^+(t) \\ \kappa^- & \text{if } \mathbf{x} \in \Omega^-(t) \end{cases}, \quad \mathcal{D} = \mathcal{D}(\mathbf{x}, t) = \begin{cases} \mathcal{D}^+ & \text{if } \mathbf{x} \in \Omega^+(t) \\ 0 & \text{if } \mathbf{x} \in \Omega^-(t) \end{cases} \quad (7)$$

Equations (1)-(4) are completed with the standard boundary conditions of prescribed velocities and surface tractions in the mechanical problem, prescribed temperature and prescribed normal heat flux in the thermal problem and prescribed fuel release into the gaseous phase in the species problem.

4 ACCOUNTING FOR GASIFICATION EFFECTS

The effect of gasification can be introduced by adding a (nonlinear) energy loss term in Eq. (3). This term represents the energy that migrates from the fluid to the gas due to the gasification of a part of the material during the heating process. The gasification heat flux has the following form

$$q_{gas} = \mathbf{H}\varepsilon_{\mathbf{v}} \quad \text{in } \Omega^- \quad (q_{gas} = -\mathbf{H}\varepsilon_{\mathbf{v}} \quad \text{in } \Omega^+) \quad (8)$$

with \mathbf{H} being the heat of gasification and

$$\varepsilon_v = f(T) \quad (9)$$

where $f(T)$ expresses the relation between the volume variation ε_v due to the temperature and the temperature itself. In our work the following Arrhenius function is chosen [6].

$$f(T) = -\rho A e^{-E/RT} \quad (10)$$

The computed mass loss of the fluid has to be included in the problem to ensure that the volume variation of the sample is correctly modeled, and thus this term is added to the right hand side of Eq.(1) ($-\varepsilon_v$ in Ω^+ and $+\varepsilon_v$ in Ω^-).

5 COMBUSTION PROBLEM

In the present study, the polymer/air reactive system is modelled as a simplified one-step chemical reaction between the fuel (F) and oxidizer (O) to generate the product (P)



where s is the stoichiometric ratio[7]. These species are identified by their mass fraction Y as follows: Y_F , Y_O and Y_P . The species reaction rates w_k are all related to the single-step reaction rate[8, 9]

$$w_m = -\mathbf{B} \frac{1}{T^2} Y_f Y_o e^{-(E/RT)} \quad (12)$$

where B and E/R are appropriate constants and T is the temperature. The oxidizer and product reaction rate are linked to the fuel reaction rate by:

$$w_O = (s)w_m \quad (13)$$

$$w_P = (1 + s)w_m \quad (14)$$

and the heat release per unit volume from combustion is scaled according to

$$Q = -w_m \Delta H \quad \text{in } \Omega^+ \quad (15)$$

where ΔH is the heat of combustion. The value of Q is introduced as a source term in Eq. (3).

6 SPATIAL AND TIME DISCRETIZATION

Numerical solutions to equations (1-4) are obtained using an Updated Lagrangian procedure. Applying the Backward Euler method to integrate in time Equations (1-4), multiplying these equations by test functions and integrating over the domain, the resulting nonlinear system of equations is solved iteratively. A Picard iteration is used for the linearization of all equations, leading to a relatively simple fixed point type solution procedure [10].

7 NUMERICAL EXAMPLES

The PFEM procedure described in this paper has been tested in two examples: 1) the melting and dripping of a polymer slab and 2) the burning of a candle in a closed container. These examples show the capability of the PFEM to handle interfaces with changes in topology due to melting, dripping and combustion.

7.1 Melting and flow of a rectangular slab

In this example a rectangular polymeric sample is mounted upright and exposed to uniform heating on one face from a radiant panel on one face. The dimensions of the sample are 10 cm high by 2.5 cm thick. The heated side is defined as a interface between the air and the polymer, and is subject to radiative and convective losses. The sample is insulated on its lateral and rear faces.

Material properties except for viscosity are taken as constant, with values as given in [11]. Figure 4 shows snapshots of the time evolution of the melt flow into the catch pan using a steady heat flux, and results for the mass loss rate are plotted in Figure 5 .

7.2 Combustion of vertical and horizontal candle

The problem considered here is a two-dimensional burning rod inside a closed container, as illustrated in Figure 6a. For simplicity, we will refer to this object as a “candle”. The dimensions of the candle are 50 cm high by 5 cm thick. From time $t = 0$ to $t = 10$ s, the temperature at the candle top is set to 950 K. In the solid phase, the processes of heating and gasification take place. Simultaneously, in the gas phase chemical processes are initiated, and temperature, fuel and oxidizer concentration gradients develop. Figures 6 to 8 show snapshots of the temperature evolution and of the flame zone in time for all configurations. Notice that as the flame grows (see Fig. 7-8)) the combustion takes place in a larger area. Finally, the flame is extinguished, first in the configuration in Fig. 6 and later in the other examples, when reactions stop due to the particles of non-oxygenated air returning to the combustion zone.

7.3 Combustion of vertical and horizontal candle accounting for melting and dripping effects

In the next example, the material properties for the candle are the same as in the previous example. Temperature increases in the candle due to combustion cause the viscosity to decrease by several orders of magnitude [11]. This induces the melting and flow of the candle material in the heated zone. The melt flows down along the heated face of the sample and drips onto the surface below. Figures 9 and 10 show the progressive melting of the candle exposed to the heat from combustion, along with the change of the flame shape.

The dripping material transports the flame(see Fig.9c) and continues burning on the surface below. After some seconds, the candle falls down and the flame is extinguished.

8 CONCLUDING REMARKS

The PFEM is a powerful technique to model the combustion, melting, flow and flame spread of thermoplastic objects in fire situations. The method allows the tracking of the motion of the polymer particles as they burn, melt, flow over the surface of the object, and fall toward and on the underlying floor. The PFEM can describe the spread of the flame onto the floor for different ambient temperature conditions and effects of gasification, in-depth absorption and radiation. The simulation of a burning candle has shown the potential of the PFEM to model the drastic change of shape of objects as they melt, drip and spread, including self-contact situations.

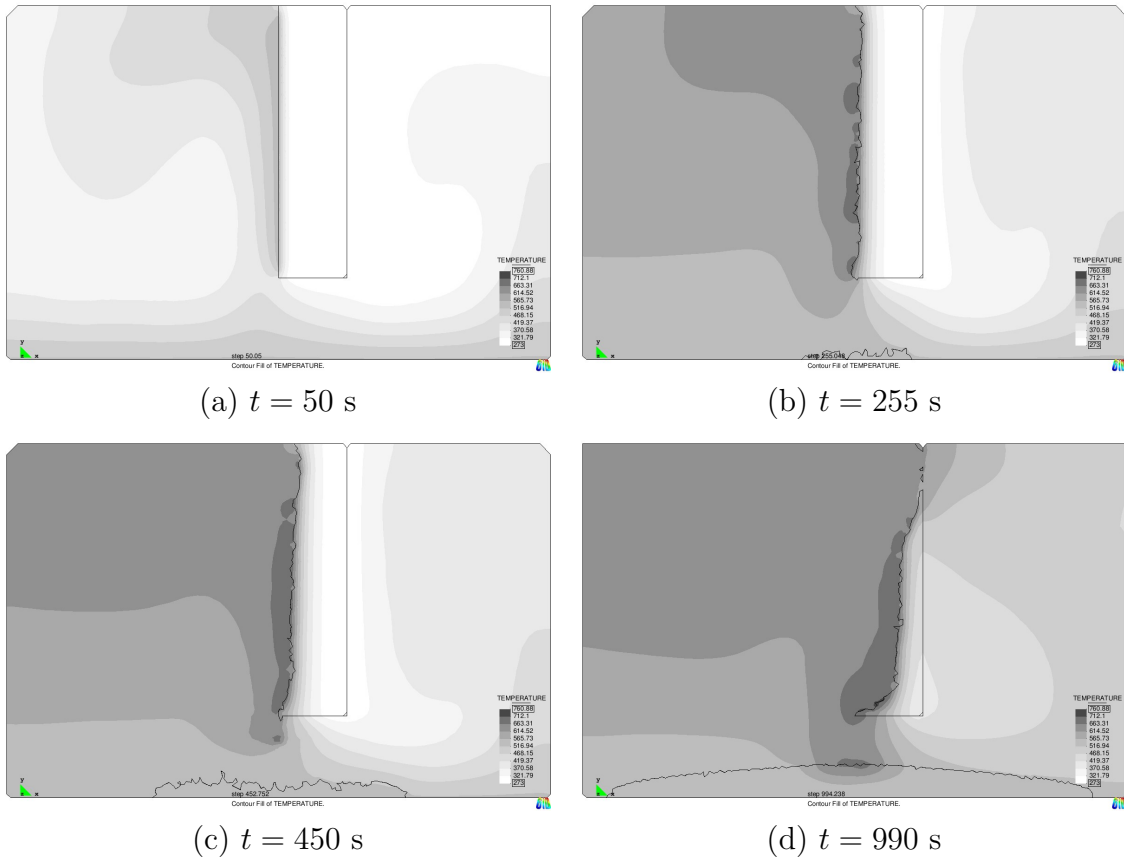


Figure 4: Evolution of the melt flow into the catch pan.

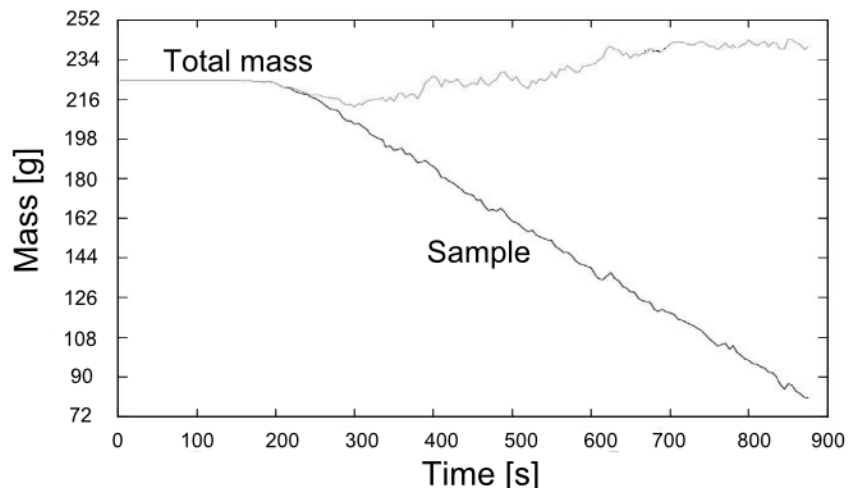


Figure 5: Mass vs time for polymer in sample and total mass.

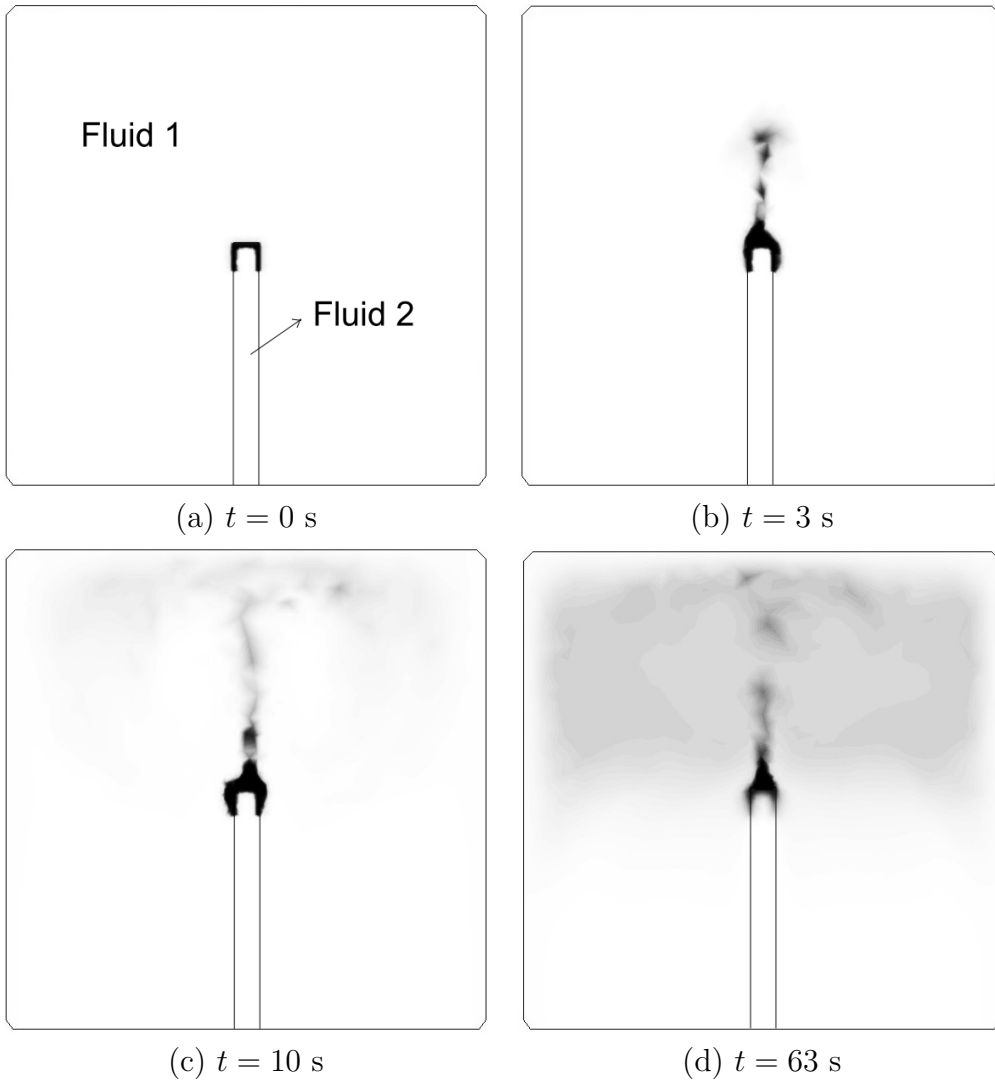


Figure 6: Temperature evolution in the combustion of a vertical (bottom-up) candle.

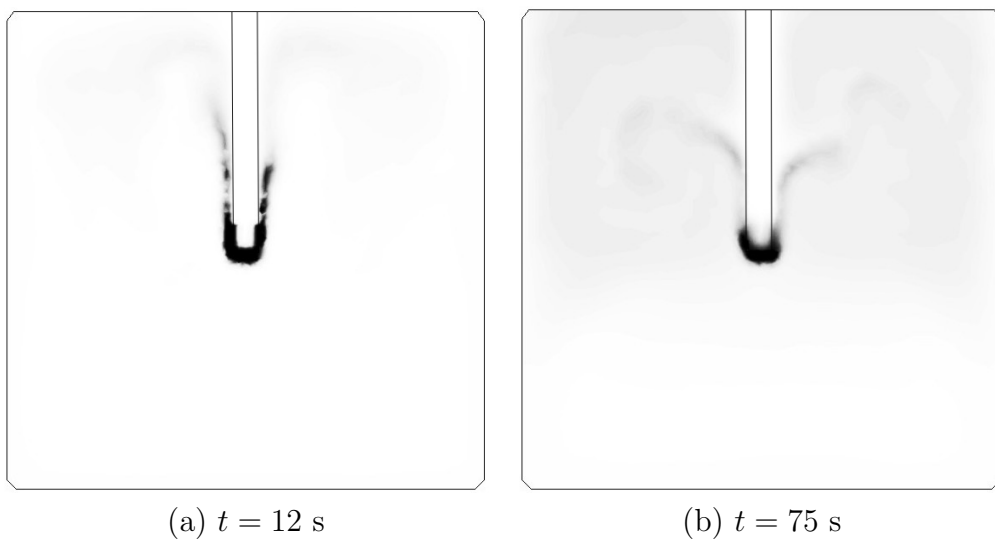


Figure 7: Temperature evolution in the combustion of a vertical (top-down) candle.

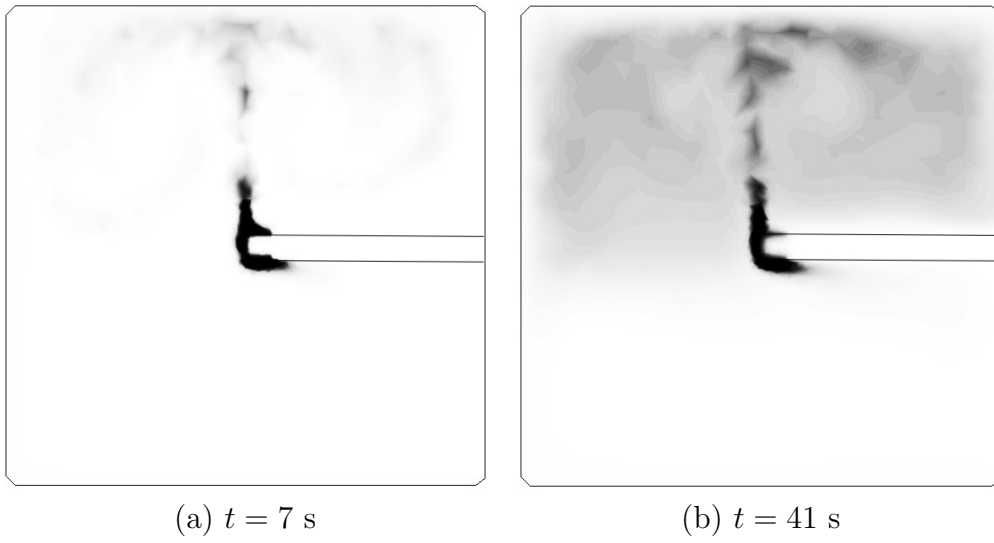


Figure 8: Temperature evolution in the combustion of a horizontal candle.

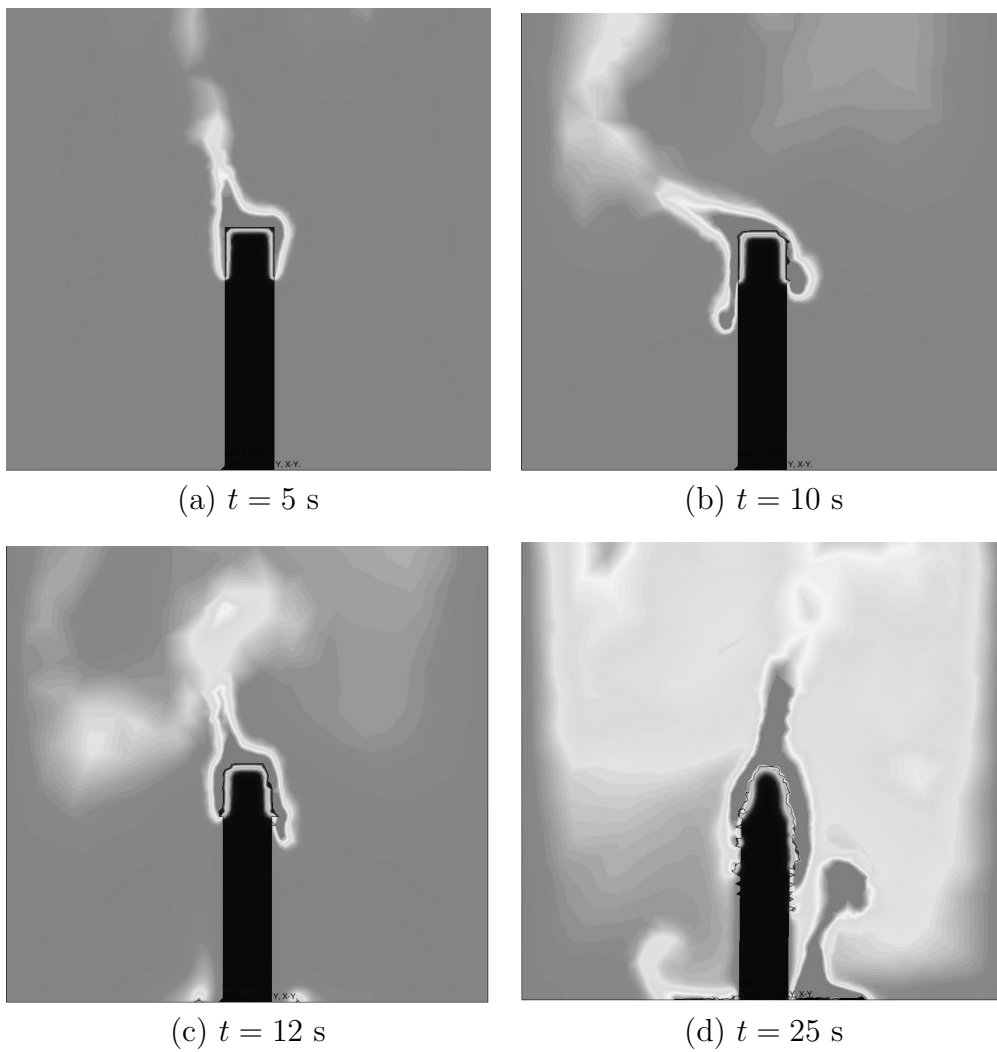


Figure 9: Combustion, melting and dripping of a candle: temperature evolution.

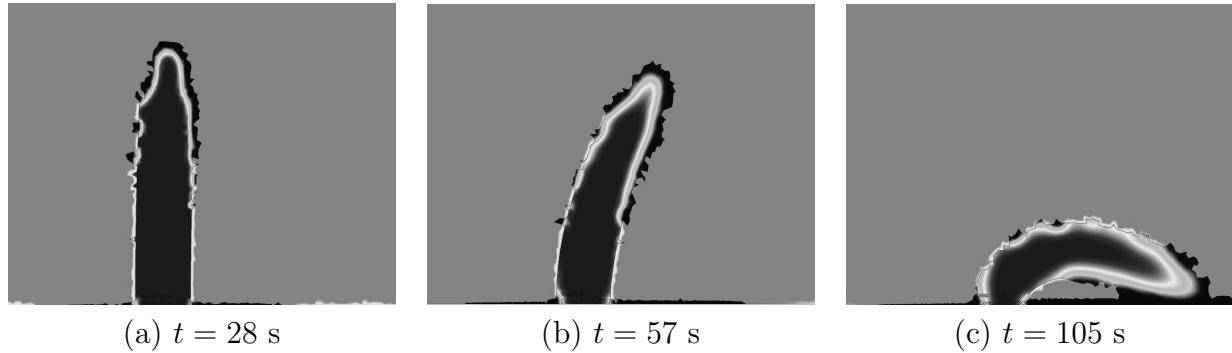


Figure 10: Combustion, melting and dripping of a candle: viscosity evolution.

Acknowledgements J. Marti thanks Dr. V. Novozhilov from University of Ulster for his advice during this research. Support from the European Commission and the European Research Council through the “Real Time Computational Techniques for Multi-Fluid Problems” project is also gratefully acknowledged.

REFERENCES

- [1] Idelsohn S.R., Marti J., Limache A. and Oñate E., Unified Lagrangian formulation for elastic solids and incompressible fluids: Application to fluid-structure interaction problems via the PFEM, *Computer Methods in Applied Mechanics and Engineering*, Vol.197, 2008, pp. 1762-1776.
- [2] Idelsohn S.R., Oñate E. and Del Pin F., The Particle Finite Element Method: A powerful tool to solve incompressible flows with free-surfaces and breaking waves, *International Journal for Numerical Methods in Engineering*, Vol. 61, 2004, pp. 964–989, 7.
- [3] Idelsohn S.R., Calvo N. and Oñate E., Polyhedrization of an arbitrary 3D point set, *Computer Methods in Applied Mechanics and Engineering*, Vol.192, 2003, pp. 2649-2667.
- [4] www.cimne.com/pfem/
- [5] Oñate E., Idelsohn S.R., Del Pin F. and Aubry R., The particle finite element method. An overview, *International Journal for Numerical Methods in Engineering*, Vol.1, No. 2, 2004, pp. 267 - 307.
- [6] Fernandez-Pello A., Flame spread modeling. *Combustion Science and Technology*, Vol. 39, 1984, pp. 119-134.
- [7] Poinso T. and Veynante D., *Theoretical and Numerical Combustion*, Second Edition.
- [8] Baek S.W., King T.Y. and Kaplan C.R., Ignition phenomenon of solid fuel in a confined rectangular enclosure, *Int.J. Heat Mass Transfer*, Vol.40, No.1, 1997, pp. 89-99.
- [9] Xie W. and Desjardin P.E., An embedded upward flame spread model using 2D direct numerical simulations, *Combustion and Flame*, Vol.156, 2009, pp. 522-530.

- [10] Marti J., The Particle Finite Element Method in Fluid-Structure Interaction, PhD thesis, FICH, UNL, Santa Fe, Argentina, (2008).
- [11] Oñate E., Rossi R., Idelsohn S.R. and Butler K., Melting and spread of polymers in fire with the Particle Finite Element Method, *International Journal for Numerical Methods in Engineering*, Vol.81, 2009, pp. 1046 - 1072.